48| Perform chloroform extraction on the supernatant from Step 47, as described in Step 19, and ethanol precipitation by adding 0.3 μl glycogen (20 mg ml^{-1}) and 150 μl ethanol, keep it on dry ice for 5 min, centrifuge it at 18,000*g* for 5 min at 4 °C, discard the supernatant and rinse the precipitate with 70% ethanol, before allowing it to air dry. Dissolve the DNA precipitate in 2 μl water.
■ PAUSE POINT The DNA solution can be stored at −20 °C for several months.

49| Add 2 μl ligation high to the sample.

50| Incubate the mixture at 16 °C for 4 h.
■ PAUSE POINT The incubation can be extended up to 16 h.

Filling in and adding A nucleotide to concatamers ● TIMING **2.5 h**

51| Prepare the following mixture (*Taq* mix) 20 min before the end of the ligation reaction: 76 μl water, 10 μl of 10× ammonium (NH_4) buffer (supplied with BIOTAQ DNA polymerase), 3 μl of 50 mM magnesium chloride ($MgCl_2$) (supplied with BIOTAQ DNA polymerase), 10 μl of 2 mM dNTPs and 1 μl BIOTAQ DNA polymerase.

52| Incubate the *Taq* mix at 95 °C for 10 min and then keep it at 72 °C.

53| Transfer the ligation mixture (from Step 50) to the *Taq* mix (from Step 52).

54| Incubate the resulting mixture at 72 °C for 30 min.

55| Perform ethanol precipitation by adding 15 μl of 10 M ammonium acetate and 250 μl ethanol, keep it on dry ice for 5 min, centrifuge it at 18,000*g* for 5 min at 4 °C, discard the supernatant and rinse the precipitate with 70% ethanol, before allowing it to air dry. Dissolve the DNA precipitate in 5 μl of 2× loading buffer.
■ PAUSE POINT The DNA solution can be stored at −20 °C for several months.

Casting the 10% polyacrylamide gel ● TIMING **~1.5 h**

56| Mix 2.5 ml of 40% acrylamide mix (acrylamide:bis-acrylamide ratio of 29:1), 1 ml of 10× TBE, 6.4 ml water, 100 μl of 10% APS and 5 μl TEMED for a gel with dimensions of 0.1 × 8.5 × 7 cm^3. Leave the gel at room temperature for >1 h to polymerize.
▲ CRITICAL STEP The freshly prepared 10% APS and TEMED should be added last, immediately before pouring the gel.

Size selection of concatamers ● TIMING **10 h**

57| Subject the gel to a constant current of 20 mA for 10 min in 1× TBE.

58| Wash the wells of the gel with 1× TBE. Apply 5 μl sample prepared in Step 55 and a 1-kb DNA ladder to the gel. Perform electrophoresis at a constant current of 20 mA until the bromophenol blue reaches the middle of the gel.

59| Separate the marker and sample lanes and wrap the gel portion containing the sample in plastic film wrap.

60| Stain the marker lane with EtBr for 5–10 min, remove excess stain by incubation with 1× TBE, and wrap the gel portion in plastic film wrap. Photograph the stained gel portion aligned with a ruler.

61| Mark the plastic film containing the sample lane at the position corresponding to 500 bp with a red pen.

62| Excise the piece of the gel containing DNA molecules of >500 bp.

63| Stain the remaining piece of gel for confirmation of concatamer formation. If successful, a ladder should be observed in the region corresponding to <500 bp (**Fig. 4**).
? TROUBLESHOOTING

64| Chop the excised piece of gel and transfer the fragments to a D-Tube moistened with water. Fill The D-Tube with 1× TBE.

65| Transfer the assembly to a submarine electrophoresis apparatus filled with 1× TBE.

66| Perform electrophoresis at a constant voltage of 100 V for 4 h.

67| Harvest the solution and subject it to ethanol precipitation by adding 0.3 μl glycogen (20 mg ml^{-1}), 25 μl of 3 M sodium acetate (pH 5.2) and 500 μl ethanol, keep it on dry ice for 5 min, centrifuge it at 18,000*g* for 5 min at 4 °C, discard the supernatant and rinse the precipitate with 70% ethanol, before allowing it to air dry. Dissolve the DNA precipitate in 2.4 μl water.
■ PAUSE POINT The DNA solution can be stored at −20 °C for several months.

© 2007 Nature Publishing Group http://www.nature.com/natureprotocols

Cloning of the size-selected concatamers ● TIMING **4.5 h**

68| Add 0.6 μl pGEM-T Easy and 3 μl ligation high to 2.4 μl of the size-selected concatamers (from Step 67).

69| Incubate the mixture at 16 °C for 4 h. The resulting product is the miRNA library.

■ PAUSE POINT The incubation can be extended up to 16 h.

Examination of the quality of the library ● TIMING **Depends on the number of plasmids to be analyzed, 4 d for 96 plasmids**

70| Transform DH5alpha with 0.5 μl library according to the manufacturer's instructions.

71| Prepare plasmid DNA from the transformants, and check the insert size by digesting the DNA with *Not*I restriction endonuclease. Determine the sequence of the inserts to verify whether miRNA sequences are included in the library (quality check).

? TROUBLESHOOTING

72| If the quality of the library is sufficient, proceed with large-scale sequencing.

73| From the sequence reads, determine the sequences of the 20–25 bp regions (in red/green on **Fig. 5**) between the sequences of the 5′- and 3′-PCR primers (adaptor sequences shown in black on **Fig. 5**), to obtain miRNA sequence and determine expression profiles.

● TIMING

Steps 1–3, casting the denaturing 15% polyacrylamide gel and preparing RNA samples: ~2.5 h
Steps 4–20, size selection of small RNAs: ~16 h
Steps 21–23, dephosphorylation of size-selected RNA molecules: 1 h
Steps 24–27, ligation of 3′ adaptor to RNA molecules: 1.5 h
Steps 28–31, RT and the SMART reaction: 1.5 h
Steps 32–35, PCR amplification of small RNA-derived cDNAs: 4.5 h
Step 36, casting the 10% polyacrylamide gel: ~1.5 h
Steps 37–43, purification of PCR amplification products: 10 h
Steps 44–50, concatamer formation: 8 h
Steps 51–55, filling in and adding A nucleotide to concatamers: 2.5 h
Step 56, casting the 10% polyacrylamide gel: ~1.5 h
Steps 57–67, size selection of concatamers: 10 h
Steps 68 and 69, cloning of the size-selected concatamers: 4.5 h
Steps 70–73, examination of the quality of the library: depends on the number of plasmids to be analyzed, 4 d for 96 plasmids

? TROUBLESHOOTING

Troubleshooting advice can be found in **Table 1**.

TABLE 1 | Troubleshooting table

Step	Problem	Possible reasons	Solution
12	Smear is observed between tRNA and 24-nt position	RNA is damaged	Begin with fresh tissue or cells Use fresh reagents to ensure they are RNase free Treat electrophoresis apparatus with 0.4 N sodium hydroxide for 30 min to remove RNase
39	Only two bands of ~70 and ~120 bp and a smear between them are observed	The amount of starting material is small	This is a common problem when the amount of RNA used as a starting material is small or recovery rate of small RNA from a gel at Step 14 is low. Given that 90 to 95-bp products should exist within the smear, excise the corresponding region based on the positions of the size markers. This process may result in excision of a fraction of incorrect size, but it is safe also to cut out portions of the gel above and below this region. Treat the three pieces of gel in parallel in the subsequent steps. Sequencing will reveal which region contains molecules of the correct size
63	Ladder is not observed	Region of the gel cut out at Step 39 is too broad	Restart from Step 32 with care to excise the 90 to 95-bp region at Step 39

© 2007 Nature Publishing Group http://www.nature.com/natureprotocols

TABLE 1 | Troubleshooting table (continued).

Step	Problem	Possible reasons	Solution
71	Only 5′ and 3′ adaptor sequences are obtained without any cDNA sequence	PCR by-products of ~70 and ~120 bp contaminate the region of the gel excised in Step 39	Given that the abundance of the adaptor dimer (~70-bp band) and trimer (~120-bp band) is much greater than that of the ~90-bp products, excise only the region of the gel corresponding to the 90 to 95-bp region, without inclusion of the dimer and trimer bands. Extending the electrophoresis time or use of a larger gel may increase the separation of the dimer and trimer from the ~90-bp products
		Ligation of small RNAs and 3′ adaptor does not work	To ensure that all reactions are working well, it is recommended to include 0.2 μg of 24-nt RNA oligomer at Step 5 in parallel with a sample. If the reaction is working, discrete 94-bp band can be observed at Step 39 and multiple sequences of 24-nt RNA oligomer are read by sequencing at Step 71
	Average length of the inserts or percentage of insert positive clones is less than desired	Small concatamer is recovered at Step 62. Recovery rate of PCR product at Step 41 or of the concatamer at Step 66 is poor	Restart from Step 32 using remaining sample of Step 31. To improve average insert length, extend the electrophoresis time at Step 58 or use of a larger gel may increase the separation of <500-bp concatamer. To improve the percentage of insert positive clones, two times scale of experiment can be performed from Step 32 to Step 43, then dissolve the precipitate at Step 43 with 43 μl of water in total. After that, proceed following steps as a single experiment scale

ANTICIPATED RESULTS

High-quality starting materials and successful handling result in recovery of 80–100% of plasmids containing inserts of >500 bp. Nucleotide sequencing typically reveals two to nine small-RNA sequences for each read. An example of such a sequence is shown in **Figure 5**. The authors recommend scientists to start with a control experiment where mRAP is conducted directly on a synthetic 24-nt RNA oligomer RNA. In such experiment, PCR amplification of miRNA-derived cDNAs should yield only the cDNA–adaptor complex at Step 39, but not other dimers or trimers in **Figure 3**. Another appropriate control experiment is to perform mRAP on a sequentially diluted small RNA samples isolated from the same cell line, as shown in our initial report for mRAP[36]. A small-scale sequencing of mRAP products from 1,000, 100 or 10 ng of starting RNAs will clarify whether mRAP has been acceptably performed.

ACKNOWLEDGMENTS We thank laboratory members for discussion as well as Mika Otani, Kyoko Nakamura and Sayaka Aoyagi for help in preparation of the manuscript. The present work was supported in part by a grant for Third-Term Comprehensive Control Research for Cancer from the Ministry of Health, Labor and Welfare of Japan, and by a grant for Scientific Research on Priority Areas 'Applied Genomics' from the Ministry of Education, Culture, Sports, Science and Technology of Japan.

Published online at http://www.natureprotocols.com
Reprints and permissions information is available online at http://npg.nature.com/reprintsandpermissions

1. Filipowicz, W. RNAi: the nuts and bolts of the RISC machine. *Cell* **122**, 17–20 (2005).
2. Hammond, S.M. Dicing and slicing: the core machinery of the RNA interference pathway. *FEBS Lett.* **579**, 5822–5829 (2005).
3. Hannon, G.J. RNA interference. *Nature* **418**, 244–251 (2002).
4. Mattick, J.S. & Makunin, I.V. Small regulatory RNAs in mammals. *Hum. Mol. Genet.* **14**, R121–R132 (2005).
5. Lee, Y., Jeon, K., Lee, J.T., Kim, S. & Kim, V.N. MicroRNA maturation: stepwise processing and subcellular localization. *EMBO J.* **21**, 4663–4670 (2002).
6. Lee, Y. *et al.* The nuclear RNase III Drosha initiates microRNA processing. *Nature* **425**, 415–419 (2003).
7. Hutvágner, G. *et al.* A cellular function for the RNA-interference enzyme Dicer in the maturation of the let-7 small temporal RNA. *Science* **293**, 834–838 (2001).
8. Ketting, R.F. *et al.* Dicer functions in RNA interference and in synthesis of small RNA involved in developmental timing in *C. elegans*. *Genes Dev.* **15**, 2654–2659 (2001).
9. Lagos-Quintana, M., Rauhut, R., Lendeckel, W. & Tuschl, T. Identification of novel genes coding for small expressed RNAs. *Science* **294**, 853–858 (2001).
10. Lau, N.C., Lim, L.P., Weinstein, E.G. & Bartel, D.P. An abundant class of tiny RNAs with probable regulatory roles in *Caenorhabditis elegans*. *Science* **294**, 858–862 (2001).
11. Lee, R.C. & Ambros, V. An extensive class of small RNAs in *Caenorhabditis elegans*. *Science* **294**, 862–864 (2001).
12. Pasquinelli, A.E. *et al.* Conservation of the sequence and temporal expression of let-7 heterochronic regulatory RNA. *Nature* **408**, 86–89 (2000).
13. Grishok, A. *et al.* Genes and mechanisms related to RNA interference regulate expression of the small temporal RNAs that control *C. elegans* developmental timing. *Cell* **106**, 23–34 (2001).
14. Knight, S.W. & Bass, B.L. A role for the RNase III enzyme DCR-1 in RNA interference and germ line development in *Caenorhabditis elegans*. *Science* **293**, 2269–2271 (2001).
15. Bernstein, E. *et al.* Dicer is essential for mouse development. *Nat. Genet.* **35**, 215–217 (2003).
16. Yang, W.J. *et al.* Dicer is required for embryonic angiogenesis during mouse development. *J. Biol. Chem.* **280**, 9330–9335 (2005).
17. Lee, R.C., Feinbaum, R.L. & Ambros, V. The *C. elegans* heterochronic gene lin-4 encodes small RNAs with antisense complementarity to lin-14. *Cell* **75**, 843–854 (1993).
18. Wightman, B., Ha, I. & Ruvkun, G. Posttranscriptional regulation of the heterochronic gene lin-14 by lin-4 mediates temporal pattern formation in *C. elegans*. *Cell* **75**, 855–862 (1993).
19. Zhao, Y., Samal, E. & Srivastava, D. Serum response factor regulates a muscle-specific microRNA that targets Hand2 during cardiogenesis. *Nature* **436**, 214–220 (2005).
20. Zhao, Y. *et al.* Dysregulation of cardiogenesis, cardiac conduction, and cell cycle in mice lacking miRNA-1-2. *Cell* **129**, 303–317 (2007).
21. He, L. *et al.* A microRNA polycistron as a potential human oncogene. *Nature* **435**, 828–833 (2005).

© 2007 Nature Publishing Group http://www.nature.com/natureprotocols

22. Hayashita, Y. *et al.* A polycistronic microRNA cluster, miR-17-92, is overexpressed in human lung cancers and enhances cell proliferation. *Cancer Res.* **65**, 9628–9632 (2005).
23. Lagos-Quintana, M. *et al.* Identification of tissue-specific microRNAs from mouse. *Curr. Biol.* **12**, 735–739 (2002).
24. Cummins, J.M. *et al.* The colorectal microRNAome. *Proc. Natl. Acad. Sci. USA* **103**, 3687–3692 (2006).
25. Mineno, J. *et al.* The expression profile of microRNAs in mouse embryos. *Nucleic Acids Res.* **34**, 1765–1771 (2006).
26. Liu, C.G. *et al.* An oligonucleotide microchip for genome-wide microRNA profiling in human and mouse tissues. *Proc. Natl. Acad. Sci. USA* **101**, 9740–9744 (2004).
27. Miska, E.A. *et al.* Microarray analysis of microRNA expression in the developing mammalian brain. *Genome Biol.* **5**, R68 (2004).
28. Thomson, J.M., Parker, J., Perou, C.M. & Hammond, S.M. A custom microarray platform for analysis of microRNA gene expression. *Nat. Methods* **1**, 47–53 (2004).
29. Nelson, P.T. *et al.* Microarray-based, high-throughput gene expression profiling of microRNAs. *Nat. Methods* **1**, 155–161 (2004).
30. Babak, T., Zhang, W., Morris, Q., Blencowe, B.J. & Hughes, T.R. Probing microRNAs with microarrays: tissue specificity and functional inference. *RNA* **10**, 1813–1819 (2004).
31. Sun, Y. *et al.* Development of a micro-array to detect human and mouse microRNAs and characterization of expression in human organs. *Nucleic Acids Res.* **32**, e188 (2004).
32. Barad, O. *et al.* MicroRNA expression detected by oligonucleotide microarrays: system establishment and expression profiling in human tissues. *Genome Res.* **14**, 2486–2494 (2004).
33. Lu, J. *et al.* MicroRNA expression profiles classify human cancers. *Nature* **435**, 834–838 (2005).
34. Chen, C. *et al.* Real-time quantification of microRNAs by stem-loop RT-PCR. *Nucleic Acids Res.* **33**, e179 (2005).
35. Tang, F. *et al.* 220-plex microRNA expression profile of a single cell. *Nat. Protoc.* **1**, 1154–1159 (2006).
36. Takada, S. *et al.* Mouse microRNA profiles determined with a new and sensitive cloning method. *Nucleic Acids Res.* **34**, e115 (2006).
37. Mano, H. & Takada, S. mRAP, a sensitive method for determination of microRNA expression profiles. *Methods* **43**, 118–122 (2007).
38. Ronaghi, M. Pyrosequencing sheds light on DNA sequencing. *Genome Res.* **11**, 3–11 (2001).

© 2007 Nature Publishing Group http://www.nature.com/natureprotocols

Leukemia (2007), 1–4
© 2007 Nature Publishing Group All rights reserved 0887-6924/07 $30.00
www.nature.com/leu

LETTER TO THE EDITOR

MicroRNA expression profiles of human leukemias

Leukemia advance online publication, 8 November 2007;
doi:10.1038/sj.leu.2405031

MicroRNAs (miRNAs) are small noncoding RNAs of 20–24 nucleotides (nt) that negatively regulate the translation of target mRNAs through incomplete base-pairing with their 3′-untranslated regions.[1] Evidence indicates that miRNAs play an important role in the development of human cancers including leukemias, with one of the most well-characterized examples being association of miR-15a and miR-16a with chronic lymphocytic leukemia. Almost half of chronic lymphocytic leukemia patients harbor a chromosome deletion that encompasses 13q14, a region that includes the genes for miR-15a and miR-16a, and the abundance of these miRNAs is reduced in chronic lymphocytic leukemia cells with the chromosome deletion.[2] Several other miRNAs, such as miR-155 and miR-17-92, have also been implicated in the pathogenesis of lymphoma.[3] It is therefore important that the entire miRNA repertoire of clinical specimens be characterized and compared among various hematologic malignancies.

Reliable assessment of the global expression profiles of miRNAs, especially for the small amounts of clinical specimens available, is not straightforward, however. Microarray-based detection of miRNAs is prone to the generation of false-positive data that may result from mishybridization of probes, although improvements have recently been developed for this technology.[4] A large-scale cloning strategy would be an ideal approach to reliable estimation of the expression level of miRNAs, provided that a sufficient number of clones were to be analyzed. However, conventional methods for isolation of miRNAs require $>10\,\mu g$ of total RNA, which is not always obtainable from clinical specimens.

We recently developed a sensitive method, mRAP (micro RNA amplification profiling)[5] that readily allows the isolation of miRNA clones from $\leqslant 1 \times 10^4$ cells. To examine the miRNA expression profiles for leukemias with mRAP, we first purified $CD34^+$ cells from individuals ($n=12$) with *de novo* acute myeloid leukemia, acute myeloid leukemia secondary to myelodysplastic syndrome, acute lymphoid leukemia or biphenotypic acute leukemia (Table 1). Column affinity-chromatography to isolate $CD34^+$ cells yielded 10–50% of the input cells with a purity of $\geqslant 90\%$ as judged by flow cytometry (data not shown). As a normal control, we also purified a $CD34^+$ cell fraction from bone marrow mononuclear cells of a healthy volunteer. Then mRAP procedure was applied to 1.1×10^6–1.0×10^8 of the purified $CD34^+$ cells from each individual in order to obtain short RNA clones.

Sequencing and computer filtering[5] of the mRAP amplicons identified a total of 38 858 qualified reads for the 13 study subjects. BLAST analysis then isolated 32 867 reads that match the human genome sequence (ncbi 36 assembly), among which 2054 reads were mapped to transfer RNA genes, 2720 to ribosomal RNA genes and 9474 to repetitive sequences. From the remaining sequences, we identified 7191 reads corresponding to 143 independent known miRNAs (Supplementary Table 1). We further searched for candidate sequences corresponding to novel miRNAs whose surrounding genome sequences (of ~100 nt) potentially fold into a hairpin structure with a single notch. In this analysis, we did not exclude miRNA candidates that were not detected in the genomes of other species, given that some miRNAs are species-specific or have arisen recently during evolution.[6]

We isolated an unexpectedly large number ($n=170$) of independent candidates for novel miRNAs among 296 sequence reads (Supplementary Table 1, Supplementary Data). The proportion of reads for such novel candidate miRNAs among all miRNA reads ranged from 1.7 to 9.5% per sample (mean, 4.7%). Of the 170 candidates, 19 were identified in at least two samples, supporting the notion that they are *bona fide* miRNAs. The surrounding genome sequence for one such candidate (designated Hsj_376) is conserved among human, cow and hedgehog (Figure 1a). Hsj_376 was found in two acute myeloid leukemia samples (corresponding to a total of 52 reads) in our data set and folds into a single hairpin (Figure 1a). In contrast, we obtained only one read for a candidate miRNA (Hsj_41) whose surrounding genome sequence also folds into a single hairpin structure (Figure 1b). However, this read was independently identified in our experiments performed both in Japan and in the Netherlands. The nucleotide sequence of all the miRNA candidates and their flanking sequences are presented in Supplementary Data.

The genomic sequences for some of the candidate miRNAs mapped in the vicinity ($\leqslant 20$ kbp) of those for other miRNAs in the human genome. For example, the gene for one candidate (Hsj_360) and hsa-miR-560 are present on the long arm of chromosome 2 separated by a distance of ~1 kbp (Supplementary Figure 1). In this instance, the genome sequences for the two miRNAs are not conserved in other species, indicative of recent evolution.

Expression of some of the candidate miRNAs was confirmed by northern blot analysis with small RNA fractions isolated from

Table 1 Clinical characteristics of the study subjects

ID (no.)	*Age (years)*	*Sex*	*Sample origin*	*Disease*	*Karyotype*
3	64	M	PB	ALL	46,XY,t(9;22)
4	45	M	BM	AML (M4)	46,XY,inv(16)
7	78	F	BM	MDS-derived AML	46,XX
10	21	F	PB	AML (M0)	46,XX,t(9:15)
12	58	M	BM	AML (M2)	46,XY
32	43	M	BM	AML (M2)	46,XY,t(8;21)
33		M	PB	AML (M1)	46,XY
44	71	M	PB	MDS-derived AML	46,XY,t(8:21)
46	61	M	PB	AML (M2)	46,XY
47	61	M	BM	AML (M3)	46,XY,t(15;17)
48	29	M	PB	BAL	46,XY
49	58	M	PB	MDS-derived AML	46,XY

Abbreviations: ALL, acute myeloid leukemia; AML, acute lymphoid leukemia; BAL, biphenotypic acute leukemia; MDS, myelodysplastic syndrome; BM, bone marrow; F, female; M, male; PB, peripheral blood.

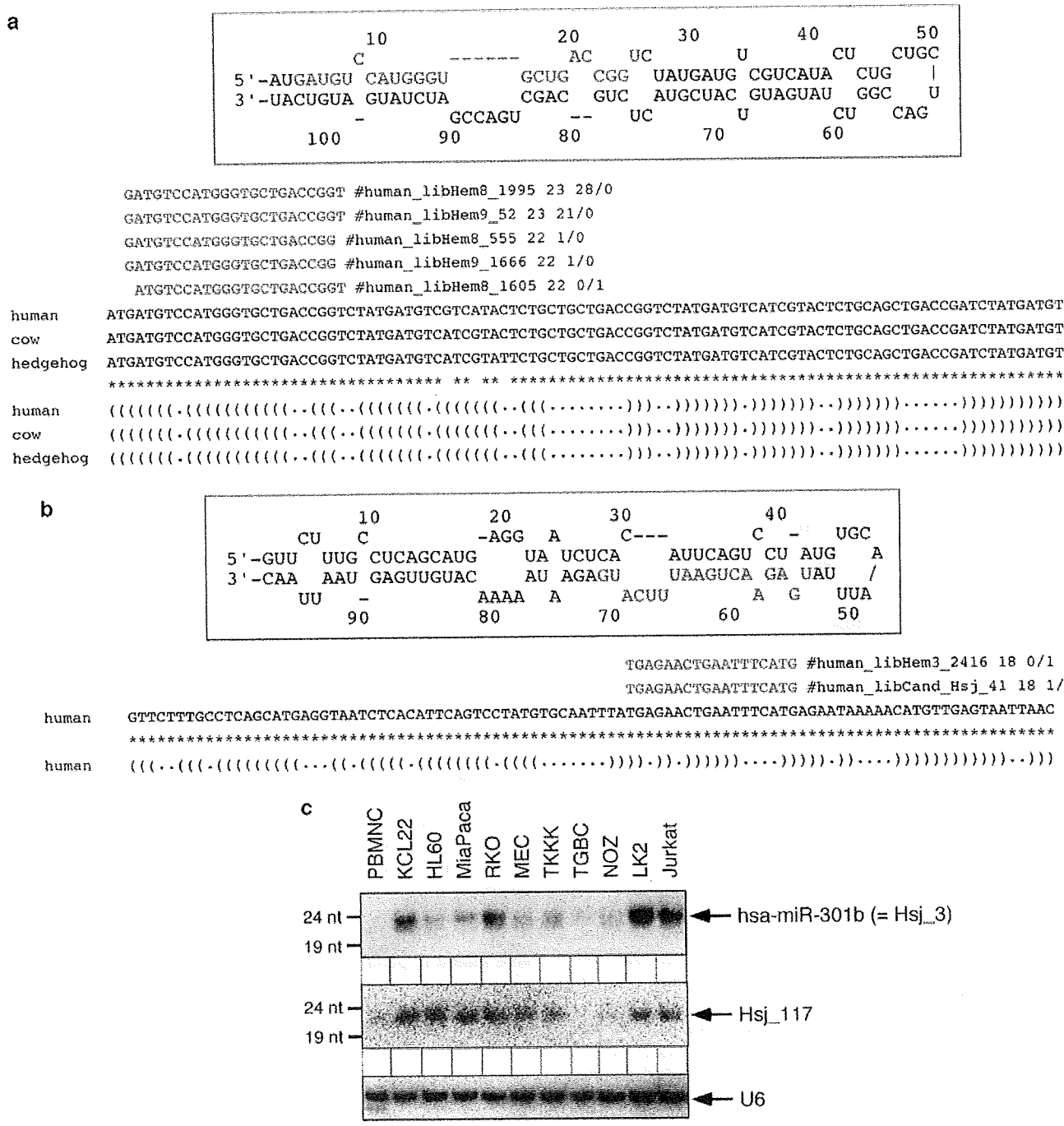

Figure 1 Nucleotide sequence and expression of novel miRNA candidates. Nucleotide sequences (red) of genes for the predicted novel miRNAs Hsj_376 (**a**) and Hsj_41 (**b**) are aligned with genomic sequences of human and other species. Asterisks indicate conserved nucleotides. Possible base-pairing schemes for the respective miRNA precursors are shown in the upper insets. (**c**) Small-RNA fractions (800 ng per lane) purified from the indicated cell lines with the use of a mirVana RNA isolation kit (Ambion, Austin, TX, USA) were subjected to northern blot analysis with 'locked' nucleic acid probes for the candidate miRNAs Hsj_3 or Hsj_117 or for U6 small nuclear RNA (internal control). Hjs_3 has been very recently deposited into the miRBase database as hsa-miR-301b. The positions of 24- and 19-nt size markers are indicated on the left. miRNA, microRNA.

a variety of human cancer cell lines, including KCL22 (chronic myeloid leukemia), HL60 (acute myeloid leukemia), MiaPaCa (pancreatic carcinoma), RKO (colorectal carcinoma), MEC (cholangiocarcinoma), TKKK (intrahepatic bile duct carcinoma), TGBC (gallbladder carcinoma), NOZ (gallbladder carcinoma), LK2 (lung squamous cell carcinoma) and Jurkat (T-cell leukemia) (Figure 1c).

The relative expression profile of miRNAs was then calculated for each sample as shown in Figure 2. Whereas some miRNAs, such as miR-124a, miR-142, miR-143 and miR-146a, were expressed in different types of leukemia, most miRNAs were expressed in a sample-specific manner. For instance, miR-29b was abundant in only two samples (ID nos. 46 and 47), with the reads for this miRNA accounting for <1% of all miRNA reads in

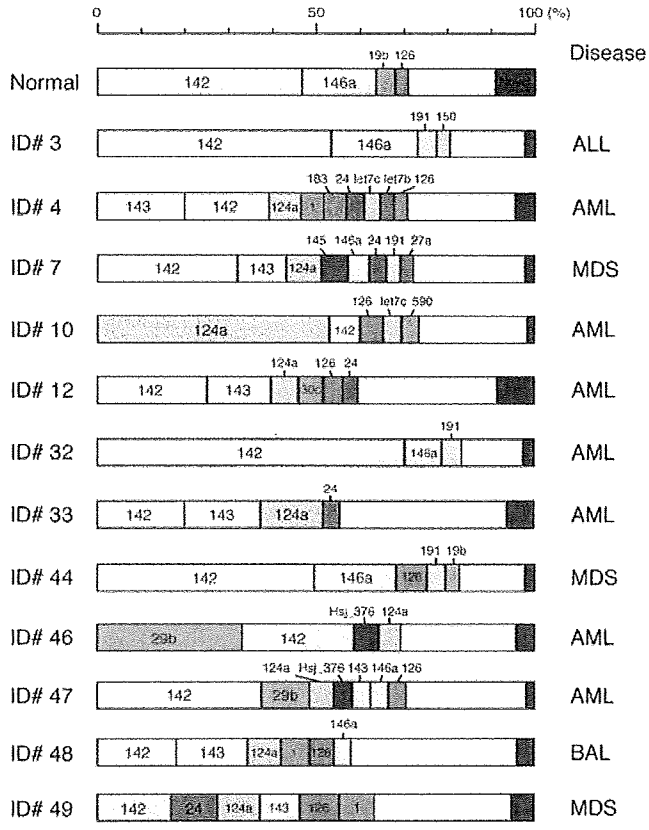

Figure 2 Expression profiles of miRNAs in CD34$^+$ specimens. The percentage contribution of each miRNA to the total miRNA population was calculated for each study subject. Abundant miRNAs are represented as color-coded, with candidates for novel miRNAs shown in red. The disease type of each individual is also indicated on the right. ALL, acute myeloid leukemia; AML, acute lymphoid leukemia; MDS, myelodysplastic syndrome; miRNA, microRNA.

each of the other specimens. Similarly, the novel miRNA candidate Hsj_376 was abundant in the same two samples but not in the others. Both hsa-miR-183 and hsa-miR-590 were detected in only single samples (ID nos. 4 10, respectively).

To examine further the similarities and differences in the miRNA profiles among the study subjects, we performed a hierarchical clustering analysis for the subjects based on the expression patterns of all known and novel miRNAs (Figure 3a). Leukemia specimens with a normal karyotype were clustered in the same branch, indicative of a relative homogeneity of these samples, at least with regard to miRNA expression. Nevertheless, the healthy volunteer was placed in a different branch, suggesting that leukemic blasts with a normal karyotype possess a miRNA profile distinct from that of nonleukemic CD34$^+$ cells with a normal karyotype.

We further attempted to identify miRNAs whose expression level was significantly linked to blast karyotype. Application of Student's *t*-test to the miRNA expression data with a Benjamini and Hochberg false discovery rate [7] of <0.05 resulted in the isolation of six miRNAs (hsa-miR-29c, hsa-miR-124a, hsa-miR-150, hsa-miR-183, hsa-miR-382 and hsa-miR-590). Hierarchical clustering of the study subjects based on the expression profiles of these 'karyotype-associated miRNAs' revealed that the healthy volunteer was again placed apart from the leukemic patients with a normal karyotype.

In conclusion, application of the mRAP procedure to CD34$^+$ leukemic blasts yielded 7487 reads for potential miRNA clones. We previously showed that mRAP readily allows the isolation of $>1\times10^6$ miRNA concatamers from $\leqslant1\times10^4$ cells and is thus suitable for miRNA profiling of clinical specimens.[5] Indeed, mRAP functioned well with the small number of purified specimens in the present study, with the result that sequencing capacity, rather than specimen quantity, is likely to be the limiting factor for the size of the final data set in most studies.

Although, in the present study, the total number of sequence reads per sample (average = 2989 reads) was not high, we were able to discover a relatively large number ($n=170$) of novel miRNA candidates from our sequence reads. Candidates for novel miRNAs continue to be identified, making it likely that the total number of human miRNAs has not yet reached saturation.[8] Our results show that CD34$^+$ leukemic blasts express a wider range of miRNAs than previously appreciated and that overall miRNA expression profiles generally reflect blast karyotype. Such karyotype-specific miRNAs may play a role in the malignant transformation of blasts of the corresponding karyotype, a possibility that needs to be confirmed by analysis of a large number of samples.

It is possible that some of the miRNA candidates identified in our study are not genuine miRNAs but rather degradation products of RNA or DNA. We believe, however, that a substantial proportion of the candidate miRNAs are indeed novel miRNAs because (i) many of them were identified in different samples in different laboratories (in Japan and in the Netherlands), (ii) many of them (together with the surrounding sequences in the genome) are conserved across various species and (iii) the expression of some of them was confirmed by northern blot analysis.

We have identified 170 novel miRNA candidates in, and demonstrated a high level of diversity in miRNA profiles among, leukemic blasts. Our data thus suggest that the miRNA repertoire of human leukemias has not yet been exhausted, and they should provide a framework for future studies in this regard.

Note added in proof

Hsj_117 and Hsj_360 have the miRBase accession numbers hsa-miR-590 and hsa-miR-663b, respectively.

Acknowledgements

This study was supported in part by a grant for Third-Term Comprehensive Control Research for Cancer from the Ministry of Health, Labor, and Welfare of Japan as well as by a grant for Scientific Research on Priority Areas 'Applied Genomics' from the Ministry of Education, Culture, Sports, Science and Technology of Japan. The authors declare no competing financial interests.

S Takada[1], Y Yamashita[1], E Berezikov[2], H Hatanaka[1], S-i Fujiwara[1], K Kurashina[1], H Watanabe[1], M Enomoto[1], M Soda[1], YL Choi[1] and H Mano[1,3]

[1]*Division of Functional Genomics, Jichi Medical University, Shimotsukeshi, Tochigi, Japan;*

[2]*Hubrecht Institute, Utrecht, The Netherlands and*

[3]*CREST, Japan Science and Technology Agency, Saitama, Japan*

E-mail: hmano@jichi.ac.jp

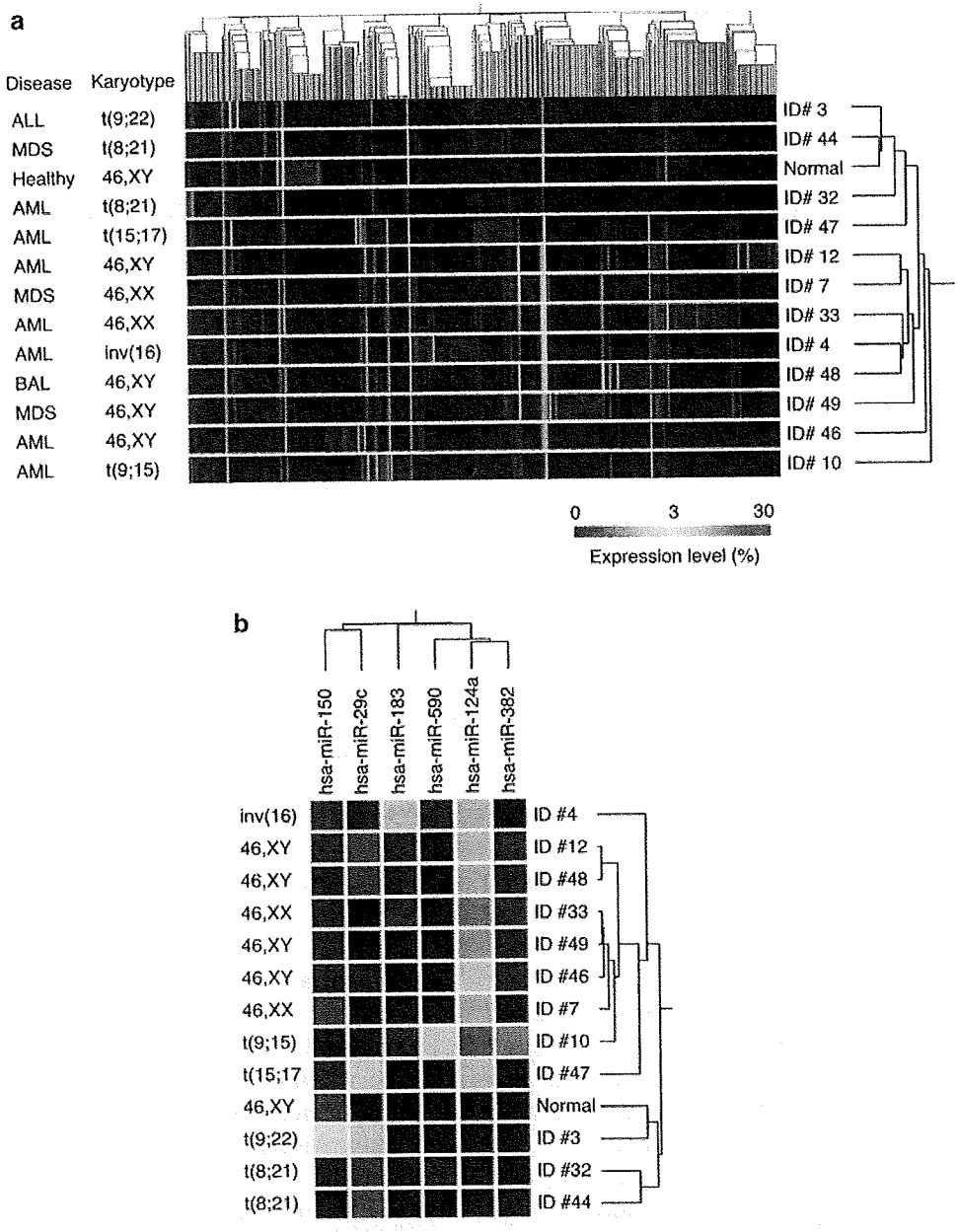

Figure 3 Hierarchical clustering of the study subjects based on miRNA expression profiles. (**a**) Subject tree generated by two-way clustering analysis with the expression profiles of all known and novel miRNAs. Each row corresponds to a separate sample, and each column to a miRNA whose expression is color-coded according to the indicated scale. The disease type and karyotype of each subject are shown at the left. (**b**) Six karyotype-associated miRNAs identified with Student's *t*-test and a false discovery rate of <0.05 were used for two-way clustering analysis as in (**a**). ALL, acute myeloid leukemia; AML, acute lymphoid leukemia; BAL, biphenotypic acute leukemia; MDS, myelodysplastic syndrome; miRNA, microRNA.

References

1 Bartel DP. MicroRNAs: genomics, biogenesis, mechanism, and function. *Cell* 2004; **116**: 281–297.
2 Calin GA, Dumitru CD, Shimizu M, Bichi R, Zupo S, Noch E *et al.* Frequent deletions and down-regulation of micro-RNA genes miR15 and miR16 at 13q14 in chronic lymphocytic leukemia. *Proc Natl Acad Sci USA* 2002; **99**: 15524–15529.
3 He L, Thomson JM, Hemann MT, Hernando-Monge E, Mu D, Goodson S *et al.* A microRNA polycistron as a potential human oncogene. *Nature* 2005; **435**: 828–833.
4 Nelson PT, Baldwin DA, Scearce LM, Oberholtzer JC, Tobias JW, Mourelatos Z. Microarray-based, high-throughput gene expression profiling of microRNAs. *Nat Methods* 2004; **1**: 155–161.
5 Takada S, Berezikov E, Yamashita Y, Lagos-Quintana M, Kloosterman WP, Enomoto M *et al.* Mouse microRNA profiles determined with a new and sensitive cloning method. *Nucleic Acids Res* 2006; **34**: e115.
6 Berezikov E, Thuemmler F, van Laake LW, Kondova I, Bontrop R, Cuppen E *et al.* Diversity of microRNAs in human and chimpanzee brain. *Nat Genet* 2006; **38**: 1375–1377.
7 Reiner A, Yekutieli D, Benjamini Y. Identifying differentially expressed genes using false discovery rate controlling procedures. *Bioinformatics* 2003; **19**: 368–375.
8 Berezikov E, Guryev V, van de Belt J, Wienholds E, Plasterk RH, Cuppen E. Phylogenetic shadowing and computational identification of human microRNA genes. *Cell* 2005; **120**: 21–24.

Supplementary Information accompanies the paper on the Leukemia website (http://www.nature.com/leu)

Cancer Chemother Pharmacol (2007) 60:189–195
DOI 10.1007/s00280-006-0360-0

ORIGINAL ARTICLE

Phase II study of weekly chemotherapy with paclitaxel and gemcitabine as second-line treatment for advanced non-small cell lung cancer after treatment with platinum-based chemotherapy

Kiyoshi Mori · Yukari Kamiyama · Tetsuro Kondo · Yasuhiko Kano · Tetsuro Kodama

Received: 7 July 2006 / Accepted: 14 September 2006 / Published online: 10 November 2006
© Springer-Verlag 2006

Abstract
Purpose We evaluated the tolerability and activity of the combination of weekly paclitaxel (PTX) and gemcitabine (GEM) in second-line treatment of advanced non-small cell lung cancer (NSCLC) after treatment with platinum-based chemotherapy.
Patients and methods PTX (100 mg/m^2) and GEM (1,000 mg/m^2) were administered to patients with previous treated NSCLC on days 1 and 8 every 3 weeks.
Results A total of 40 patients (performance status 0/1/2, 7/27/6 pts) were enrolled. The response rate was 32.5% (95% confidence interval: 18.0–47.0%). The median survival time was 41.7 weeks (95% confidence interval: 28.5–54.7 weeks). The median time to disease progression was 19 weeks. Hematological toxicities (grade 3 or 4) observed included neutropenia in 60%, anemia in 15%, and thrombocytopenia in 12.5% of patients. Non-hematological toxicities were mild, with the exception of grade 3 diarrhea, pneumonitis, and rash in one patient each. There were no deaths due to toxicity.
Conclusion The combination of weekly PTX and GEM is a feasible, well-tolerated, and active means of second-line treatment of advanced NSCLC.

Keywords Non-small cell lung cancer · Second-line chemotherapy · Weekly chemotherapy · Gemcitabine · Paclitaxel

K. Mori (✉) · Y. Kamiyama · T. Kondo · Y. Kano · T. Kodama
Department of Thoracic Diseases, Tochigi Cancer Center, 4-9-13, Yonan, Utsunomiya, Tochigi 320-0834, Japan
e-mail: kmori@tcc.pref.tochigi.jp

Y. Kamiyama
e-mail: ykamiyam@tcc.pref.tochigi.jp

T. Kondo
e-mail: tkondo@tcc.pref.tochigi.jp

Y. Kano
e-mail: ykano@tcc.pref.tochigi.jp

T. Kodama
e-mail: tkodama@tcc.pref.tochigi.jp

Introduction

The clinical usefulness of second-line chemotherapy has been established for cases of advanced non-small cell lung cancer (NSCLC) in which tumor has recurred or exhibits resistance to treatment after first-line chemotherapy. The effectiveness of docetaxel, pemetrexed, and elrotinib for second-line chemotherapy for NSCLC has been demonstrated in phase III clinical studies [13, 23, 24]. Furthermore, paclitaxel (PTX) and gemcitabine (GEM) have been shown to be effective against NSCLC resistant to platinum preparations [5, 16, 20]. There appears to be partial non-cross-resistance between these drugs and platinum preparations.

In previous attempts at second-line chemotherapy for NSCLC, the response rate was 0–38% for patients treated with PTX alone at intervals of 3 weeks [12, 21, 25] and 8–37.5% for patients treated with low-dose weekly PTX therapy [5, 16, 26, 28]. On the other hand, the rate of response to uncombined GEM therapy was 6–21% [7, 11, 17, 20, 22].

In combined PTX and GEM therapy, the two drugs exhibit interactions with each other but no overlap or synergism of adverse reactions. When this combined

regimen was applied to previously untreated patients with NSCLC, the response rate was high, at 29–46% [1, 3, 4, 8, 15, 18]. When a combination of PTX (administered every 3 weeks) and GEM was used for second-line chemotherapy, the response rate was either 18 or 39% [2, 14].

Weekly chemotherapy for lung cancer has recently been attempted at several facilities [3, 9]. Favorable results of weekly chemotherapy have also been reported for recurrent NSCLC [5, 16, 26, 28]. Compared to standard regimens of chemotherapy, with administration of drugs at intervals of 3–4 weeks, weekly chemotherapy has certain advantages. For example, the single dose level of anti-cancer drugs can be reduced with weekly chemotherapy, and the dose level can be adjusted after the start of treatment depending on signs of hematological toxicity of the drugs or the general condition of individual patients. In comparison with treatment at intervals of 3–4 weeks, weekly chemotherapy was of equal efficacy but had fewer side effects [3]. Weekly chemotherapy is thus a promising means of treating cases of recurrent NSCLC in which bone marrow function has been compromised by first-line chemotherapy.

The present study was undertaken to evaluate the effectiveness and safety of weekly chemotherapy using a combination of PTX and GEM in cases of advanced NSCLC in which tumor had recurred or relapsed after platinum-based first-line chemotherapy or platinum-based first-line chemotherapy had failed to exert efficacy.

Patients and methods

Patient selection

Patients were required to have histologically or cytologically confirmed non-resectable or metastatic NSCLC that had progressed during or after one or more chemotherapy regimens. The trial was initiated after a rest period of at least 4 weeks following previous chemotherapy (2 weeks in the case of radiotherapy). Patients were required to have recovered completely from prior therapy, and to have no ongoing toxicity greater than grade 1. Other eligibility criteria were as follows: measurable lesions; life expectancy of at least 12 weeks; Eastern Cooperative Oncology Group (ECOG) performance status ≤ 2; adequate bone marrow reserve (defined as absolute granulocyte count $\geq 2{,}000$/ml and platelet count $\geq 100{,}000$/ml); adequate hepatic and renal function (defined as serum creatinine level ≤ 2 mg/dl, AST and ALT ≤ 1.5 times the upper limit of normal, and bilirubin ≤ 1.5 mg/dl). Exclusion criteria included pre-existing motor or sensory neurological signs or symptoms $\geq$ grade 2 (Common Terminology Criteria for Adverse Events version 3.0) and active infections. Asymptomatic treated or untreated patients with brain metastases were not excluded from the study. The Ethics Committee of the Tochigi Cancer Center approved the study protocols. Written informed consent was obtained from every patient stating that the patient was aware of the investigational nature of this treatment regimen.

Treatment

Paclitaxel was administered at a dose of 100 mg/m^2 intravenously during a 1-h infusion on days 1 and 8 of the treatment cycle. Gemcitabine was administered at a dose of 1,000 mg/m^2 intravenously during a 30-min infusion on days 1 and 8 of the treatment cycle. Prior to each treatment, patients were given diphenhydramine 50 mg orally, and an H2 blocker intravenously along with dexamethasone 16 mg 30 min before PTX administration. Granisetron 3 mg was administered intravenously as an antiemetic. The length of each chemotherapy cycle was 21 days. Patients who experienced grade 4 leukopenia or neutropenia that lasted for 3 or more days, or who experienced grade 4 thrombocytopenia or reversible grade 2 neurotoxicity or liver dysfunction, received reduced doses of both PTX and GEM (PTX 80 mg/m^2, GEM 800 mg/m^2) for the next cycle. If non-hematological toxicities of grade 3 or higher occurred, treatment was stopped. Subsequent courses of chemotherapy were started after 3 weeks when the leukocyte count was 3,000/mm^3 or more, the neutrophil count was 1,500/mm^3 or more, the platelet count was 75,000/mm^3 or more, serum creatinine were less than 1.5 mg/dl, GOT and GPT were less than twice the upper limit of the normal range, and neurotoxicity was grade 1 or less. If these variables did not return to adequate levels by the first day of the next course of chemotherapy, treatment was withheld until full recovery. If more than 6 weeks passed from the time of the last treatment before these criteria were met or if change in treatment more significant than reduction of dose was indicated, the patient was removed from the study at that time, but still included in the analysis of its results.

Evaluation of responses and toxicity

Pretreatment evaluation included medical history, physical examination, complete blood count, bone marrow examination, serum biochemical analyses,

chest roentgenogram, electrocardiogram, and urinalysis. All patients underwent radionuclide bone scan, magnetic resonance or computerized tomography (CT) of the brain, and CT of the thorax and abdomen. Complete blood count, biochemical tests, serum electrolytes, urinalysis, and chest roentgenograms were obtained before patients received chemotherapy.

Responses and toxicity were evaluated on the basis of tumor images obtained by CT and other techniques, laboratory data, and subjective/objective symptoms and signs before, during, and after administration of the study drugs and during the period from completion of treatment to final analysis. Measurable disease parameters were determined every 4 weeks by various means such as computerized tomography. Evaluation was performed in compliance with the Response Evaluation Criteria in Solid Tumors (RECIST) Guidelines for antitumor activity and with Common Terminology Criteria for Adverse Events version 3.0 for safety. Patients were withdrawn from the study if evidence of tumor progression was obtained. The Institutional Ethical Review Committee gave approval to the study.

The primary endpoint of the study was the response rate. Simon's two-stage optimum design was used to determine sample size and decision criteria. It was assumed that a response rate of 30% among eligible patients would indicate potential usefulness while a rate of 10% would be the lower limit of interest, with $\alpha = 0.05$ and $\beta = 0.10$. Using these design parameters, the fist stage of the study was initially to enroll 18 patients, and this regimen was to be rejected if fewer than two patients had an objective response. If two or more patients responded, accrual was to be continued to 36 patients. Considering the percentage of probable dropout cases, 40 patients were required. Secondary endpoints were toxicity and overall survival. Response and survival rates were both calculated on an intent-to-treat basis. Overall survival and time to progression were measured from the start of this treatment up to the time of death or up to the date of the last follow-up clinical assessment. Survival curves were constructed using the Kaplan–Meier method.

Results

Patient characteristics

Forty patients were enrolled in this study from October 2000 to July 2003. All patients were assessable for toxicity, response, and survival. Characteristics of the 40 patients are listed in Table 1. All 40 patients had received a prior platinum-based chemotherapy regimen (Table 1). Two of these patients had received more than one chemotherapy regimen. All 40 patients were eligible for toxicity assessment. Four patients had received prior chemotherapy in the neoadjuvant setting. Of the 40 patients, 15 had initially responded to platinum-based therapy, 24 patients had achieved stable disease (SD), and one had progressive disease (PD).

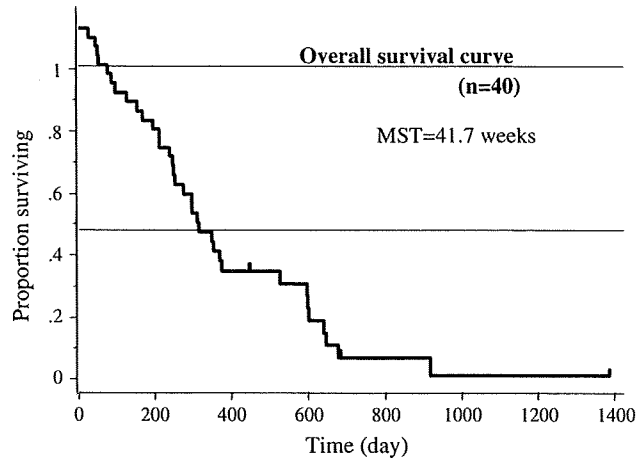

Fig. 1 Kaplan–Meier estimated overall survival curves. Median survival time, 41.7 weeks; 1-year survival rate, 38%

Efficacy of treatment

The mean number of cycles administered per patient was 4, and number of cycles ranged from one to twelve. Three patients required reduction of dose due to neutropenia and thrombocytopenia. Thirteen patients exhibited partial response (PR). Overall response rate was 32.5% (13/40) [95% confidence interval (CI): 18–47%]. SD was achieved in 26 patients (65%), and one (2%) achieved PD. All 40 patients were included in the survival analysis, with a median follow-up time of 82.9 weeks (range 56–263 weeks). The overall median survival time was 41.7 weeks (95% CI: 28.5–54.7 weeks). The 1-year survival rate was 37.5% (15/40) (Fig. 1). The median time to disease progression was 19 weeks.

Toxicities (Table 2)

Table 2 lists toxicities observed during this study. Hematological toxicities included high incidences of leukopenia and neutropenia, with leukopenia and neutropenia of grade 3 or higher occurring in 45 and 60% of patients, respectively. Anemia and thrombocytopenia of grade 3 or higher occurred in 15 and 12.5% of patients, respectively. Non-hematological toxicities

Table 1 Patient characteristics

Eligible patients	40
Gender	
Male	27
Female	13
Age (years)	
Median	59
Range	33–75
Performance status	
0	7
1	27
2	6
Histology	
Adenocarcinoma	30
Squamous cell	8
Large cell	2
Stage III	10
Stage IV	30
Number of metastatic sites	
Median	2
Range	0–3
Location of metastases	
Bone	13
Lung nodules	12
Brain	10
Lymph nodes	7
Liver	5
Adrenals	3
Subcutaneous	1
Prior surgery	4
Prior irradiation	15
Lung only	9
Brain only	4
Lung and bone	2
Prior chemotherapy	40
Cisplatin/vinorelbine	32
Cisplatin/docetaxel	5
Cisplatin/irinotecan	3
Response to prior chemotherapy	
Partial response	15
Stable disease	24
Progressive disease	1

observed included grade 3 pneumonitis in one patient, who exhibited rapid recovery following administration of steroids, grade 3 diarrhea in one, and grade 3 rash in one. Other non-hematological toxicities observed were of grade 2 or less and included nausea in 47.5%, vomiting in 20%, alopecia in 45%, sensory neuropathy in 35%, and fatigue in 32.5% of patients. All of these toxicities disappeared or were improved by symptomatic treatment. There were no deaths due to toxicity.

Discussion

Although a standard regimen of chemotherapy for recurrent NSCLC is being established, it is still important to determine how the outcome of treatment of this cancer can be improved [13, 23, 24]. At this point, the results of large-scale phase III clinical trials indicate single-agent chemotherapy with docetaxel, erlotinib, or pemetrexed as the standard chemotherapy regimen for recurrent NSCLC. In recent years, however, many reports have been published investigating two-drug combined therapy rather than single-agent therapy for recurrent NSCLC, with the objective of further improving therapeutic outcomes [2, 5, 7, 11–14, 20–26, 28].

A large number of reports have been published concerning salvage chemotherapy for recurrent NSCLC. Platinum-based chemotherapy is now used as the first-line chemotherapy at most medical facilities. Reports on second-line chemotherapy for NSCLC published to date have principally concerned uncombined drug therapy or two-drug combined therapy using non-platinum preparations [2, 5, 7, 11, 12, 14, 16, 17, 20–22, 25, 26, 28]. At several facilities, weekly administration chemotherapy has been adopted [5, 16, 26, 28]. Weekly-administration chemotherapy allows single dose levels to be reduced, thus making it possible to adjust the dose levels of anti-cancer agents after the start of treatment depending on adverse reactions or the general condition of individual patients.

Table 3 summarizes the results of two-drug combined therapy for recurrent NSCLC using non-platinum preparations [2, 6, 9, 10, 14, 19, 27]. The studies shown in this table were phase I-II in the case of that reported by Iaffaioli [14], phase III in that by Fossella [9], and phase II in the other studies. The overall response rate varied widely among studies, from 0.8 to 39%. The overall median survival time was 24–47 weeks and the one-year survival rate was 19–46%. Major adverse reactions observed in these studies were signs of hematological toxicity (particularly neutropenia), excluding the studies involving prophylactic G-CSF treatment reported by Androulakis [2] and Wachters [27]. Signs of non-hematological toxicity varied depending on the drugs used, and symptoms and signs unique to each drug were noted.

For combined PTX and GEM therapy for recurrent NSCLC, Androulakis [2] reported an overall response rate of 18%, an overall median survival time of 47 weeks, and a median time to disease progression of 34 weeks. Compared to the present study, the overall response rate reported by Androulakis was lower, while the overall median survival time and median time to disease progression were more favorable in the study by Androulakis. The dosing regimen used by Androulakis involved administration of PTX (175 mg/m^2; day 8), GEM (900 mg/m^2; days 1 and 8), and granulocyte colony-stimulating factor (G-CSF; days

Table 2 Maximum toxicity over 152 cycles (40 patients)

	CTCAE v 3.0 grade (number of patients)					Grade 3 ≤ (%)
	0	1	2	3	4	
Leukopenia	7	4	11	15	3	18 (45)
Neutropenia	6	5	5	17	7	24 (60)
Febrile neutropenia	–	–	–	2	–	2 (5)
Anemia	4	8	22	5	1	6 (15)
Thrombocytopenia	9	21	5	3	2	5 (12.5)
Pneumonitis	36	1	0	1	0	1 (2.5)
Diarrhea	27	9	3	1	0	1 (2.5)
Rash	22	15	2	1	0	1 (2.5)
Nausea	21	19	0	0	0	
Vomiting	32	3	5	0	0	
Fatigue	27	11	2	0	0	
Alopecia	22	17	1	0	0	
Neuropathy-sensory	26	14	0	0	0	
Edema	32	8	0	0	0	
Arthralgia	33	7	0	0	0	

CTCAE v 3.0 Common terminology criteria for adverse events version 3.0

Table 3 Non-platinum regimens used as second-line treatment of non-small cell lung cancer

First author (Ref.)	No. of patients	Regimen and schedule			Response rate (%)	Survival	
						Median (weeks)	1-year (%)
Androulakis [2]	49	P	175 mg/m^2	d 8 q 3w	18	47	37
		G	900 mg/m^2	d 1,8 q 3w			
		G-CSF	150 μg/m^2	d 9–15			
Iaffaioli [14]	37	P	90–240 mg/m^2	d 1 q 3w	39	40	46
		G	1,000 mg/m^2	d 1,8 q 3w			
Fossella [9]	123	FO	2 g/m^2/day	d 1–3 q 3w	0.8	24	19
		V	30 mg/m^2	d 1,8,15 q 3w			
Kosmas [19]	43	D	100 mg/m^2	d 8 q 3w	33	36	28
		G	1,000 mg/m^2	d 1,8 q 3w			
Cao [6]	33	CPT11	300 mg/m^2	d 1 q 4w	9	25	23
		V	30 mg/m^2	d 1,14 q 4w			
Georgoulias [10]	76	CPT11	300 mg/m^2	d 8 q 3w	18.4	38	24.5
		G	1,000 mg/m^2	d 1,8 q 3w			
Wachters [27]	52	CPT11	200 mg/m^2	d 1 q 3w	10	27	30
		D	60 mg/m^2	d 1 q 3w			
		G-CSF	150 μg/m^2	d 2–12			
Present study	40	P	100 mg/m^2	d 1,8 q 3w	32.5	42	38
		G	1,000 mg/m^2	d 1,8 q 3w			

P paclitaxel, *G* gem citabine, *F0* infostamide, *V* vinorebine, *D* docetaxel, *CPT-11* irinotecan, *G-CSF* granulocyte colony-stimurating factor, *d* day, *q* every

9–15), with each cycle of treatment lasting for 3 weeks. Because their regimen involved prophylactic administration of G-CSF, the incidence of grade 3 or worse neutropenia was lower than that in the present study (12 vs. 60%). However, the incidence of grade 2 or worse fatigue (a sign of non-hematological toxicity) was lower in the present study (4%) than in that reported by Androulakis (51%).

Belani [19] reported the results obtained with combined use of PTX and GEM as first-line chemotherapy for NSCLC. In their study, PTX was administered using two regimens and a comparison was made between treatment with PTX on day 1 (200 mg/m^2) and weekly treatment with PTX on days 1 and 8 (100 mg/m^2/dose; identical to the regimen used in the present study). According to their report, the response rate was 45% for the first regimen and 46% for the second regimen, the median survival time was 42 and 39 weeks and the 1-year survival rate 46 and 41% for the first and second regimens, respectively. Efficacy thus did not differ

significantly between the two regimens. Signs of hematological toxicity were the major adverse reactions observed following treatment with both regimens. The incidences of neutropenia and alopecia were lower with the weekly regimen. On the basis of these results, Belani concluded that weekly PTX treatment combined with GEM is also useful as first-line chemotherapy for NSCLC.

In conclusion, weekly chemotherapy with PTX and GEM is a tolerable and active regimen for patients with advanced NSCLC previously treated with platinum-containing chemotherapy regimens. It should be recommended as a candidate regimen in planning a phase III clinical study of NSCLC previously treated with platinum-containing chemotherapy, and will ultimately be evaluated in a phase III clinical study.

Acknowledgments This work was supported in part by a Grant-in-Aid for Cancer Research from the Ministry of Health, Labour and Welfare (Tokyo, Japan), and by the second-term comprehensive 10-year strategy for cancer control.

References

1. Aguiar D, Aguiar J, Bohn U (2005) Alternating weekly administration of paclitaxel and gemcitabine: a phase II study in patients with advanced non-small cell lung cancer. Cancer Chemother Pharmacol 55:152–158
2. Androulakis N, Kouroussis C, Kakolyris S, Tzannes S, Papadakis E, Papadimitriou C, Geroyianni A, Georgopoulou T, Dimopoulou I, Souglakos J, Kotsakis A, Vardakis N, Hatzidaki D, Georgoulias V (1998) Salvage treatment with paclitaxel and gemcitabine for patients with non-small cell lung cancer after cisplatin-or docetaxel-based chemotherapy: a multicenter phase II study. Ann Oncol 9:1127–1130
3. Belani CP, Dakhil SR, Waterhouse D, Desch C, Rooney D, Clark R, Jorge J (2002) A randomized phase II trial of gemcitabine (G) plus paclitaxel (P) vs gemcitabine plus weekly paclitaxel in the treatment of non-small cell lung cancer (NSCLC). Proc Am Soc Oncol 21:312A
4. Bhatia S, Hanna N, Ansari R, Pletcher W, Einhorn L, Ng E, Sandler A (2002) A phase II study of weekly gemcitabine and paclitaxel in patients with previously untreated stage IIIb and IV non-small cell lung cancer. Lung Cancer 38:73–77
5. Buccheri G, Ferrigno D. (2004) Second-line weekly paclitaxel in patients with inoperable non-small cell lung cancer who fail combination chemotherapy with cisplatin. Lung Cancer 45:227–236
6. Cao MG, Aramendia JM, Salgado E et al (2002) Second-line chemotherapy with irinotecan and vinorelbine in stage IIIB and IV non-small-cell lung cancer. A phase II study. Am J Clin Oncol 25:480–484
7. Crino L, Mosconi AM, Scagliotti G et al (1999) Gemcitabine as second-line treatment for advanced non-small cell lung cancer: a phase II trial. J Clin Oncol 17:2081–2085
8. Douillard JY, Lerouge D, Monnier A et al (2001) Combined paclitaxel and gemcitabine as first-line treatment in metastatic non-small cell lung cancer: a multicentre phase II study. Br J Cancer 84:1179–1184
9. Fossella FV, DeVore R, Kerr RN et al (2000) Randomized phase III trial of docetaxel versus vinorelbine or ifosfamide in patients with advanced non-small cell lung cancer previously treated with platinum-containing chemotherapy regimens. J Clin Oncol 18:2354–2362
10. Georgoulias V, Kouroussis C, Agelidou A et al (2004) Irinotecan plus gemcitabine vs irinotecan for the second-line treatment of patients with advanced non-small-cell lung cancer pretreated with docetaxel and cisplatin: a multicentre, randomized, phase II study. Br J Cancer 91:482–488
11. Gillenwater HH, Tynan M, Natoli S et al (2000) Second-line gemcitabine in refractory stage IV non-small cell lung cancer: a phase II trial. Clin Lung Cancer 2:133–138
12. Hainsworth JD, Thompson DS, Greco FA et al (1995) Paclitaxel by 1-h infusion: an active drug in metastatic non-small cell lung cancer. J Clin Oncol 13:1604–1614
13. Hanna N, Shepherd FA, Fossella FV et al (2004) Randomized phase III trial of pemetrexed versus docetaxel in patients with non-small cell lung cancer previously treated with chemotherapy. J Clin Oncol 22:1589–1597
14. Iaffaioli RV, Tortoriello A, Gravina A et al (2000) Phase I-II study of gemcitabine and paclitaxel in pretreated patients with stage IIIB-IV non-small cell lung cancer. Lung Cancer 30:203–210
15. Isla D, Rosell R, Sanchez JJ et al (2001) Phase II trial of paclitaxel plus gemcitabine in patients with locally advanced or metastatic non-small cell lung cancer. J Clin Oncol 19:1071–1077
16. Juan O, Albert A, Ordono F et al (2002) Low-dose weekly paclitaxel as second-line treatment for advanced non-small cell lung cancer: a phase II study. Jpn J Clin Oncol 32:449–454
17. Kooten MV, Traine G, Cinat G et al (1999) Single-agent gemcitabine in pretreated patients with non-small cell lung cancer: results of an Argentinean multicentre phase II trial. Br J Cancer 81:846–849
18. Kosmidis P, Mylonakis N, Dimopoulos A et al (2000) Combination chemotherapy with paclitaxel plus carboplatin versus paclitaxel plus gemcitabine in inoperable non-small cell lung cancer: a phase III randomized study. Preliminary results. Semin Oncol 27:3–8
19. Kosmas C, Tsavaris N, Vadiaka M et al (2001) Gemcitabine and docetaxel as second-line chemotherapy for patients with non-small cell lung carcinoma who failed prior paclitaxel plus platinum-based regimens. Cancer 92:2902–2910
20. Lara PN, Gumerlock PH, Mack PC et al (2004) Gemcitabine in patients with non-small cell lung cancer previously treated with platinum-based chemotherapy: a phase II California Cancer Consortium Trial. Clin Lung Cancer 6:102–107
21. Nauman C, DeLaney TF, Park J et al (1997) Paclitaxel (Taxol) as a single agent salvage therapy in non-small cell lung cancer (NSCLC). Proc Am Soc Clin Oncol 16:476A
22. Sculier JP, Lafitte JJ, Berghmans T et al (2000) A phase II trial testing gemcitabine as second-line chemotherapy for non-small cell lung cancer. Lung Cancer 29:67–73
23. Shepherd FA, Dancey J, Ramlau R, Mattson K, Gralla R, O'Rourke M, Levitan N, Gressot L, Vincent M, Burkes R, Coughlin S, Kim Y, Berille J (2000) Prospective randomized trial of docetaxel versus best supportive care in patients with non-small cell lung cancer previously treated with platinum-based chemotherapy. J Clin Oncol 18:2095–2103
24. Shepherd FA, Pereira JR, Ciuleanu T et al (2005) Erlotinib in previously treated non-small cell lung cancer. N Engl J Med 53:123–132

25. Socinski MA, Steagall A, Gillenwater H et al (1999) Second-line chemotherapy with 96 h infusional paclitaxel in refractory non-small cell lung cancer: report of a phase II study. Cancer Invest 17:181–188
26. Socinski MA, Schell MJ, Bakri K et al (2002) Second-line, low-dose, weekly Paclitaxel in patients with stage IIIB/IV non-small cell lung carcinoma who fail first-line chemotherapy with carboplatin plus paclitaxel. Cancer 95:1265–1273
27. Wachters FM, Groen HJM, Biesma B et al (2005) A randomize phase II trial of docetaxel vs docetaxel and irinotecan in patients with stage IIIb-IV non-small-cell lung cancer who failed first-line treatment. Br J Cancer 92:15–20
28. Yasuda K, Igishi T, Kawasaki Y et al (2004) Phase II study of weekly paclitaxel in patients with non-small cell lung cancer who have failed previous treatments. Oncology 66:347–352

Invest New Drugs (2007) 25:31–40
DOI 10.1007/s10637-006-9000-0

PRECLINICAL STUDIES

Cytotoxic effects of histone deacetylase inhibitor FK228 (depsipeptide, formally named FR901228) in combination with conventional anti-leukemia/lymphoma agents against human leukemia/lymphoma cell lines

Yasuhiko Kano · Miyuki Akutsu · Saburo Tsunoda · Tohru Izumi · Hiroyuki Kobayashi · Hiroyuki Mano · Yusuke Furukawa

Published online: 22 July 2006
© Springer Science + Business Media, LLC 2006

Summary FK228 is a novel antitumor depsipeptide that inhibits histone deacetylases and restores the expression of genes aberrantly suppressed in cancer cells. This agent was shown to have broad antitumor activity in preclinical studies, and is currently under phase I/II evaluations. Because of its wide spectrum of actions, it is reasonable to consider the combination with other anticancer drugs in clinical application. We studied the cytotoxic interaction of FK228 in combination with conventional antileukemic agents using human promyelocytic leukemia HL60, Philadelphia chromosome-positive (Ph^+) chronic myelogenous leukemia KU-812, T-cell lymphoblastic leukemia MOLT3 and Burkitt's lymphoma Raji cell lines. For the combination of FK228 and imatinib, Ph^+ leukemia KU812, K562 and TCC-S cell lines were used. The cells were exposed simultaneously to FK228 and other agents for 4 days. Cell growth inhibition was determined by using 3-(4,5-dimethylthiazol-2-yl)-2,5-diphenyltetrazolium bromide (MTT) assay. We used the isobologram method of Steel and Peckham to evaluate the cytotoxic interaction at the concentration of drugs that produced 80% cell growth inhibition (IC_{80}). FK228 showed an additive effect with cytarabine, carboplatin, doxorubicin, etoposide, 4-hydroperoxy-cyclophosphamide, 6-mercaptopurine and SN-38 (active metabolite of irinotecan) in all cell lines studied. FK228 with methotrexate and vincristine showed an antagonistic effect in three and one of the four cell lines, respectively. FK228 was additive with imatinib in all three Ph^+ leukemia cells. Our findings suggest that FK228 is a promising candidate for combining with most anticancer agents except for methotrexate and vincristine, which produce suboptimal effects.

Keywords FK228 · Depsipeptide · Histone deacetylase inhibitor · Antagonism · Synergism

Y. Kano · M. Akutsu · S. Tsunoda · T. Izumi · H. Kobayashi
Division of Hematology, Tochigi Cancer Center,
4-9-13 Yonan, Utsunomiya, Tochigi 320-0834, Japan

H. Mano
Division of Functional Genomics, Center for Molecular Medicine,
Jichi Medical School, 3311-1 Yakushiji,
Shimotsuke, Tochigi 329-0498, Japan

Y. Furukawa (✉)
Division of Stem Cell Regulation, Center for Molecular Medicine,
Jichi Medical School, 3311-1 Yakushiji,
Shimotsuke, Tochigi 329-0498, Japan
e-mail: furuyu@jichi.ac.jp

Introduction

Histone acetylation and deacetylation play an important role in the control of gene transcription by affecting the interaction between DNA and histones [1]. Acetylation is linked to activation of gene transcription, whereas deacetylation is associated with transcriptional repression. Both processes are catalyzed by specific enzymes, histone acetyltransferases and histone deacetylases, respectively [2].

Recent advances in molecular oncology suggest that histone deacetylation may play a role in the uncontrolled growth of cancer cells [2]. Histone deacetylase inhibitors have been observed to cause growth arrest, differentiation and apoptosis against a variety of cancer cell lines [3, 4]. Five structural classes of histone deacetylase inhibitors have been identified, including FK228, trichostatin A, MS-27-275, oxamflatin and SAHA [3, 4]. Several agents are currently under clinical investigations.

FK228, formally named FR901228, is a novel antitumor depsipeptide isolated from *Chromobacterium violaceum* [5]. FK228 inhibits histone deacetylases and causes arrest of the cell cycle in the G1 and/or G2-phase, cell differentiation and apoptosis [6]. FK228 effectively suppresses the growth of human tumor cells *in vitro*, i.e., the concentrations of FK228 required for 50% cell growth inhibition of clinical samples of chronic lymphocytic leukemia and a variety of lymphoid cell lines are much lower than those of normal hematopoietic progenitor cells [7, 8]. Small cell lung cancer cell lines resistant to etoposide, irinotecan or cisplatin are not cross-resistant to FK228 [9]. In animal studies, FK228 prolongs the survival time of mice bearing murine and human tumors [10, 11].

Phase I trials of FK228 in patients with refractory neoplasms, lymphomas and leukemias have been reported [12–14]. Three patients with cutaneous T-cell lymphoma had a partial response and one patient with peripheral T-cell lymphoma, unspecified, had a complete response [12]. On the other hand, FK228 shows limited antitumor activity in patients with chronic lymphocytic leukemia and acute myeloid leukemia, while it effectively inhibits histone deacetylase *in vivo* [14]. The dose-limiting toxicities were fatigue, nausea, vomiting, and transient thrombocytopenia and neutropenia. These results suggest that FK228 has some therapeutic effects in the treatment of cancer including lymphoma and leukemias, but, for clinical development, it is important to combine with other anticancer agents. However, cytotoxic effects of FK228 combined with commonly used antitumor agents have not been studied.

In the present study, we investigated the *in vitro* cytotoxic interactions of FK228 in combination with commonly-used anti-leukemia/lymphoma agents against human leukemia/lymphoma cell lines. The results underline the importance of the design of the combination of FK228 with other anticancer agents for clinical therapy.

Materials and methods

Cell lines

The experimental studies of FK228 in combination with standard anti-leukemic agents were conducted with human promyelocytic leukemia HL60, Ph^+ chronic myelogenous leukemia KU-812, T-cell lymphoblastic leukemia MOLT3 and B-cell Burkitt's lymphoma Raji cells. The combination of FK228 with imatinib was studied using Ph^+ leukemia, KU812, K562 and TCC-S cells. Cells were maintained in 75-cm^2 plastic tissue culture flasks containing RPMI1640 medium (Sigma Co., St. Louis, Mo., USA) supplemented with 10% heat-inactivated fetal calf serum (Sigma Co.) and antibiotics.

Drugs

FK228, SN-38 and imatinib were kindly provided by Fujisawa Pharmaceutical Co., Ltd. (Osaka, Japan), Yakult Co., Ltd. (Tokyo, Japan) and Novartis Inc. (Basel, Switzerland), respectively. Other anticancer agents used and their sources were: cytarabine (Nihon Shinyaku Co. Ltd., Tokyo), doxorubicin (Meiji Co., Ltd., Tokyo), etoposide (Nihon Kayaku Co., Ltd., Tokyo), 4-hydroperoxy-cyclophosphamide and vincristine (Shionogi Co., Ltd., Tokyo), methotrexate (Lederle Japan, Ltd., Tokyo) and 6-mercaptopurine (Sigma Co.). FK228 and Imatinib were dissolved in dimethyl sulfoxide. SN-38 was dissolved in 0.1 N NaOH. All other drugs were dissolved in RPMI1640. Appropriate concentrations of stock solutions of all drugs were stored at $-80°C$. The drugs were diluted with RPMI1640 before use.

Cell cycle analysis by flow cytometry

Cell cycle analysis was performed using KU812 and MOLT3 cells. Cells were cultured in the presence of either no drug or a variety of concentrations of FK228 for 24, 48 and 72 h. The cells were then stained with propidium iodide in preparation for flow cytometry with the FACScan/CellFIT system (Becton-Dickinson, San Jose, CA). A DNA histogram was obtained by analyzing 25,000 cells with the ModFIT program (Becton-Dickinson) [15].

Cell culture

HL60, KU812, MOLT3 and Raji cells were used for the combination studies. These cells in the logarithmic phase were harvested and resuspended in a final concentration of $0.5–2 \times 10^5$ cells/ml of fresh medium containing 10% fetal calf serum. Cell suspensions (100 μl) were dispensed into individual wells of a 96-well tissue culture plate with a lid (Falcon, Oxnard, CA). Eight plates were prepared for the testing of each drug combination. Each plate had one 8-well control column containing medium alone and one 8-well control column containing cells but no drugs. For each drug or drug combination, 8 wells were used. Cells were incubated in a humidified atmosphere of 95% air/5% CO^2 at 37°C overnight. Drug solutions of FK228 and other drugs at different concentrations were then added (50 μl) to 8 wells containing cell suspensions and the plates were incubated under the same conditions for 4 days. The final concentration of dimethyl sulfoxide in the media was less than 0.1%, and it had no effect on cell growth inhibition in our study.

MTT assay

Viable cell growth was determined by using a modified MTT assay as described previously [16].

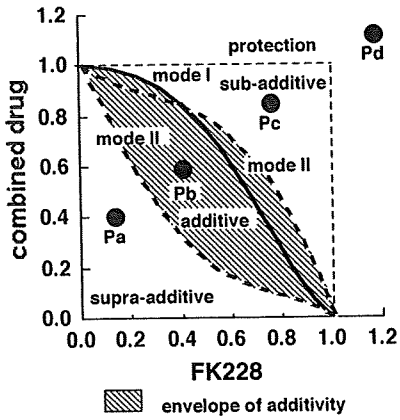

Fig. 1 Schematic representation of an isobologram. Envelope of additivity, surrounded by Mode I (solid line) and Mode II (dotted line) isobologram lines, is constructed from the dose-response curves of FK228 and a combined drug. The concentrations that produce 80% cell growth inhibition are expressed as 1.0 on the ordinate and the abscissa of isobolograms. Combined data points Pa, Pb, Pc and Pd show supra-additive, additive, sub-additive and protective effects, respectively

Isobologram method of Steel and Peckham

Cytotoxic interactions of FK228 with other agents at the point of IC_{80} were evaluated by the isobologram method of Steel and Peckham [17]. The theoretical basis of the isobologram method and the procedure for making isobolograms have been described in detail previously [18, 19].

Based upon the dose-response curves of FK228 and the other agents, three isoeffect curves were constructed (Fig. 1). If the agents were acting additively by independent mechanisms, the combined data points will lay near the Mode I line (hetero-addition). If the agents were acting additively by similar mechanisms, the combined data points will lay near the Mode II lines (iso-addition).

Since it is unknown in advance whether the combined effects of two agents will be hetero-additive, iso-additive or an effect intermediate between these extremes, all possibilities should be considered. Thus, when the data points of the drug combination fell within the area surrounded by three lines (envelope of additivity), the combination was regarded as additive. When the data points fell to the left of the envelope, i.e., the combined effect was caused by lower doses of the two agents than was predicted, we regarded the drug combination as having a supra-additive effect (synergism). When the points fell to the right of the envelope, i.e., the combined effect was caused by higher doses of the two agents than was predicted, but within the square or on the line of the square, we regarded the combination as having a sub-additive effect, i.e., the combination was superior or equal to a single agent but was less than additive. When the data points were outside the square, the combination was regarded as having a protective effect, i.e., the combination was inferior in cytotoxic action to a single agent. Both sub-additive and protective interactions were regarded as antagonism.

Data analysis

When the observed data points for the combination mainly fell in the area of supra-additivity or in the areas of sub-additivity and protection, i.e., the mean value of the observed data was smaller than that of the predicted minimum values or larger than that of the predicted maximum values, the combination was considered to have a synergistic or antagonistic effect, respectively. To determine whether the condition of synergism (or antagonism) truly existed, statistical analysis was performed. The Wilcoxon signed-ranks test was used for comparing the observed data with the predicted minimum (or maximum) values for additive effects, which were closest to the observed data (i.e. the data on the boundary (Mode I or Mode II lines) between the additive area and supra-additive area (or sub-additive and protective areas) [20]. Probability (P) values ≤ 0.05 were considered significant. Combinations with $P > 0.05$ were regarded as indicating additive/synergistic (or additive/antagonistic) effects. All statistical analyses were performed using the Stat View 4.01 software program (Abacus Concepts, Berkeley, CA).

Results

Cytotoxic effects of FK228 and conventional anticancer agents on human leukemia/lymphoma cell lines

The dose-response curves of FK228 for the HL60, MOLT3, Raji, KU812, K562, and TCC-S cells are shown in Fig. 2. The IC_{80} values of a 96-h exposure to FK228 for these cells were

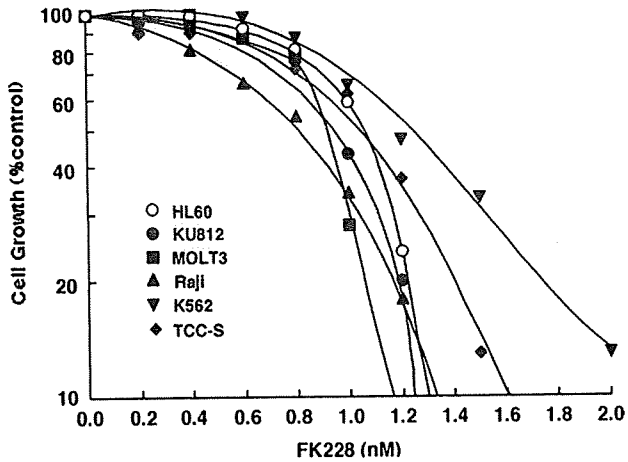

Fig. 2 Dose-response curves for FK228 in HL60, MOLT3, KU812, Raji, K562 and TCC-S cells

3.7 ± 0.2 nM, 3.6 ± 0.3 nM, 3.2 ± 0.2 nM, 3.6 ± 0.3 nM, 5.1 ± 0.2 nM, and 4.2 ± 0.4 nM, respectively (Fig. 2, Table 1), all of which are clinically achievable *in vivo* according to a recent clinical study [12]. The IC_{80} values of a 96-h exposure to other agents for these cells are also shown in Table 1.

Cell cycle analysis of FK228-treated cells

We analyzed the effects of FK228 on the cell cycle profile of leukemia cell lines. Cell cycle arrest at G1 to the early S-phase was observed in KU812 cells at 24 h of culture with FK228 at concentrations of more than 4.5 nM, followed by the induction of apoptosis at 72 h (Fig. 3). FK228, at concentrations of more than 4.5 nM, induced G1 arrest and apoptosis simultaneously after 48 h of culture in MOLT3 cells (data not shown). In contrast, FK228 arrested HL60 and K562 cells in G2/M phase of the cell cycle (data not shown, see Sutheesophon et al. [21] for detail).

Cytotoxic effects of FK228 in combination with other agents

Figure 4 shows the dose-response curves for FK228 in combination with either cytarabine or methotrexate in KU812 cells. Each isobologram was generated based on such dose-response curves.

Cytotoxic effects of FK228 in combination with cytarabine: Figure 5 shows the isobolograms of this combination in HL60, KU812, MOLT3 and Raji cells. In HL60 cells, all combined data points fell within the envelope of additivity (Fig. 5a). The mean value of the data (0.63) was larger than that of the predicted minimum values (0.12) and smaller than that of the predicted maximum values (0.89), indicating that the simultaneous exposure to FK228 and cytarabine produced an additive effect (Table 2). In MOLT3, KU812 and Raji cells, all data points also fell within the envelope of additivity, indicating that the simultaneous exposure to FK228 and cytarabine also produced an additive effect.

Cytotoxic effects of FK228 in combination with either carboplatin, doxorubicin, etoposide, 4-hydroperoxycyclophosphamide or SN-38: In all four cell lines, all or most combined data points fell within the envelope of additivity (isobolograms not shown), indicating that simultaneous exposure to FK228 and these drugs produced an additive effect (Table 2).

Cytotoxic effects of FK228 in combination with 6-mercaptopurine: Because HL60 was resistant to 6-mercaptopurine, we used other three cell lines to study this combination. In MOLT3, KU812 and Raji cells, all or most combined data points fell within the envelope of additivity (isobolograms not shown), indicating that simultaneous exposure to FK228 and 6-mercaptopurine produced an additive effect (Table 2).

Cytotoxic effects of FK228 in combination with methotrexate: Figure 6 shows the isobolograms of this combination in HL60, KU812, MOLT3 and Raji cells. In HL60, KU812 and Raji cells, all or most data points fell in the areas of sub-additivity and protection. The mean values of the observed data (0.93, 1.13 and 0.98, respectively) were larger than those of the predicted maximum additive values (0.87, 0.44 and 0.76, respectively) (Table 2). Statistical analysis showed that the difference was significant ($P < 0.05$, $P < 0.01$ and $P < 0.01$, respectively), indicating an antagonistic effect of simultaneous exposure to these two agents. In MOLT3 cells, data points fell within the envelope of additivity and in the areas of sub-additivity and protection. The mean value of the observed data (0.87) was larger than that of the predicted maximum additive values (0.86), but the difference was not statistically significant ($P > 0.05$), indicating an additive/antagonistic effect of simultaneous exposure to these two agents.

Table 1 The IC_{80} values of FK228 and combined agents for leukemia cell lines[a]

	HL60	MOLT3	Raji	KU812	K562	TCC-S
FK228 (nM)	3.7	3.6	3.2	3.6	5.1	4.2
Cytarabine (nM)	400	160	1400	8900	n.d.	n.d.
Carboplatin (μM)	7.8	5.3	15	100	n.d.	n.d.
Doxorubicin (nM)	92	15	220	25	n.d.	n.d.
Etoposide (μM)	0.44	0.25	1.3	4	n.d.	n.d.
4-Hydroperoxy-cyclophosphamide (μM)	6.2	1.3	1.4	7.4	n.d.	n.d.
6-Mercaptopurine (μM)	10	1.7	4	1.7	n.d.	n.d.
Methotrexate (nM)	25	25	70	18	n.d.	n.d.
SN-38 (nM)	8.3	0.94	2.1	27	n.d.	n.d.
Vincristine (nM)	1	0.67	2.2	1.5	n.d.	n.d.
Imatinib (nM)	n.d.	n.d.	n.d.	97	270	85

[a] Values represent the means of at least three independent experiments.

n.d. = not done.

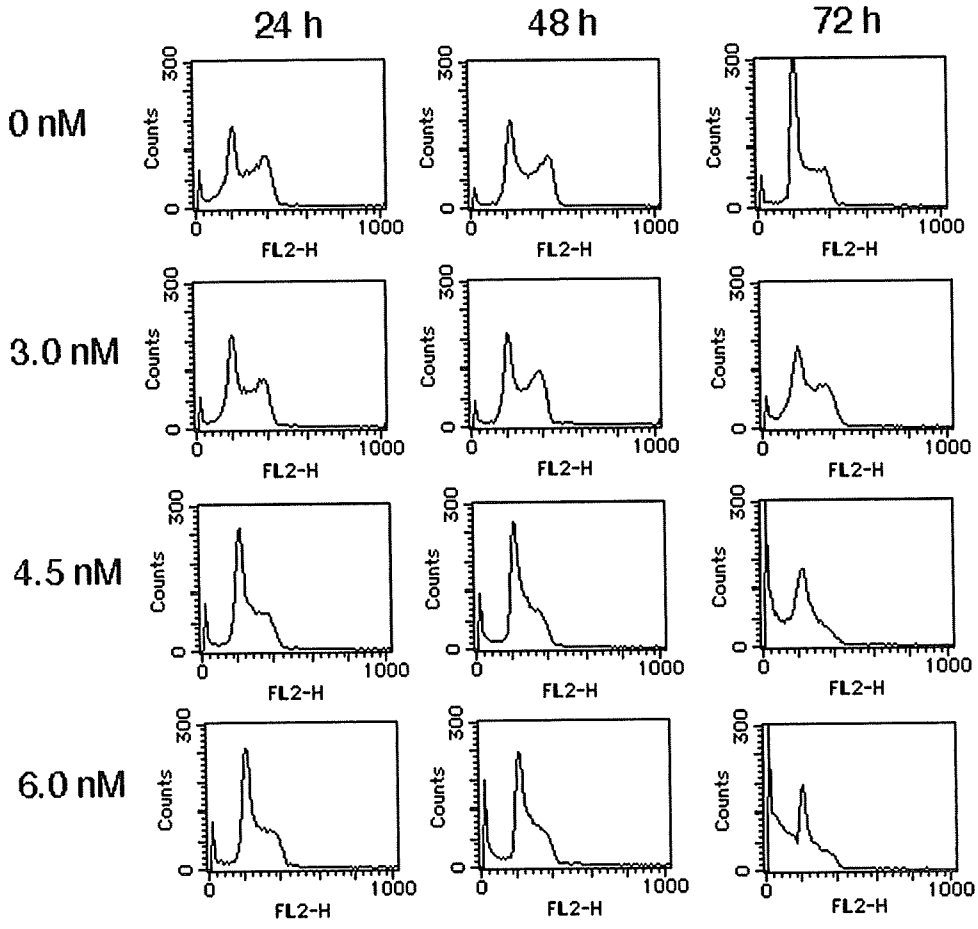

Fig. 3 Cell cycle analysis of KU812 cells treated with FK228. Cells were cultured in the absence or presence of various concentrations of FK228, and DNA histograms were obtained after 24, 48 and 72 h of culture

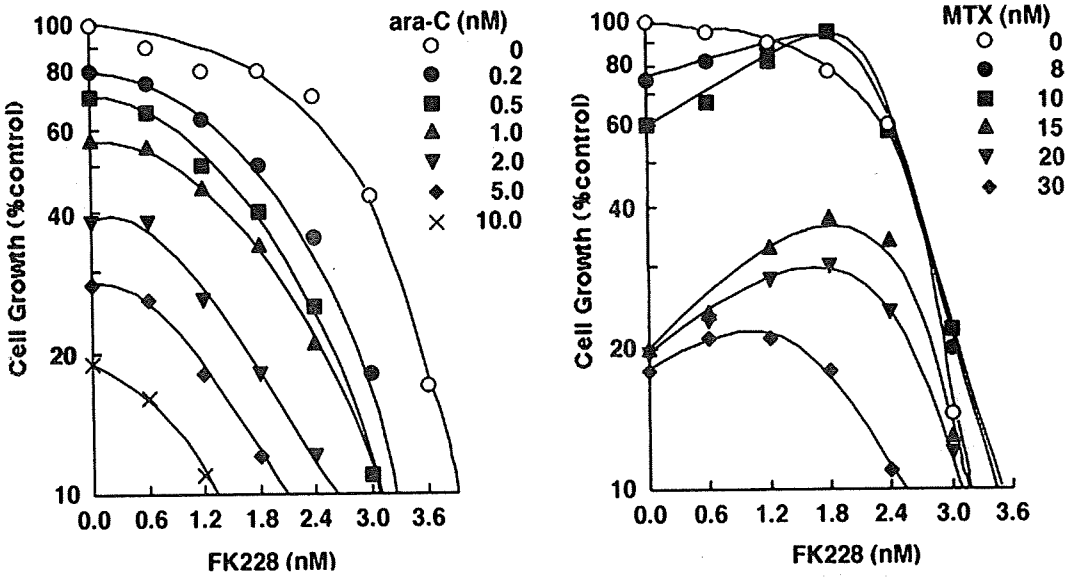

Fig. 4 Dose-response curves for FK228 in combination with cytarabine (ara-C) and methotrexate (MTX) in KU812 cells. Cell growth was measured by the MTT assay after 4 days and was plotted as a percentage of the control (cells not exposed to drugs). FK228 concentrations are shown on the abscissa. Each point represents the mean value for at least 3 independent experiments; the SEs were less than 20% and thus were omitted